Eur. Phys. J. Appl. Phys. **99**, 10 (2024)

https://doi.org/10.1051/epjap/2024230146

THE EUROPEAN PHYSICAL JOURNAL APPLIED PHYSICS

Original Article

Molarity dependence of solution on structural and hydrophobic properties of ZnO nanostructures

Zehira Belamri[1,*], Warda Darenfad[2], and Noubeil Guermat[3]

[1] Laboratory of Phase Transformation, Frères Mentouri – Constantine 1 University, 25000 Constantine, Algeria
[2] Department of Physics, Faculty of Exact Sciences, University of Constantine 1, 25000 Constantine, Algeria
[3] Department of Electronics, Faculty of Technology, University of M'sila, PO Box 166 Ichebilia, 28000 M'sila, Algeria

Received: 1 August 2023 / Accepted: 2 January 2024

Abstract. The impact of the molarity solution on this property of elaborated ZnO thin films coating on a metallic aluminum substrate are the aim of this present work. ZnO is the chosen material to be deposited in this work; it is one of the most used materials in the development of hydrophobic surfaces due to its interesting physical and structural properties. The samples were characterized by X-ray diffraction (XRD), Raman spectroscopy, scanning electron microscopy (FEG-SEM) equipped with energy dispersive X-ray analysis (EDX) and a profilometer. The wettability properties of the synthesized films were analyzed by measuring the contact angle between the surface of studied films and a deposited water drop (WCA). XRD analysis and Raman spectroscopy show that ZnO is well synthesized by thermal oxidation in this present work, where the crystallization of the deposited layer increases with increasing solution molarity. The calculated crystallite sizes are in the nanometric scale and reach their maximum value for the prepared solution of 0.3 M with an average crystallites size of 32 nm. The obtained results show that the surface morphology strongly depends on solution molarity and has an effect on the hydrophobic properties of the elaborated ZnO thin films. The elaborated sample with solution of 0.2 M shows compact granular attached to each other with an average size of 200 nm. Measured surface roughness ranges from 7.653 μm to 0.526 μm. The shape and surface roughness of the prepared thin layers had an effect on the surface hydrophobicity. The largest measured contact angle of 135.72 °, was achieved with a solution molarity of 0.2 M with the greatest roughness indicate the best hydrophobicity of this sample.

Keywords: Thin films / ZnO / nanostructure / XRD / SEM / hydrophobic

1 Introduction

Surface wettability is an important aspect of surface properties and has significant implications for various technological applications. Surfaces can be categorized based on their characteristics, including chemical composition, structure morphology, and the contact angle (CA) of liquids on the surface. Surfaces can be super hydrophilic ($0°< \theta < 5°$), hydrophilic ($5°< \theta < 90°$), hydrophobic ($90°< \theta <150°$), or superhydrophobic ($150°< \theta < 180°$). Superhydrophobic surfaces have shown potential for practical applications such as catalytic tissue engineering, self-cleaning [1], oil recovery [2], anti-adhesion [2], photocatalysis [3], antibacterial [4], micro-droplet transport, anti-icing coatings [5], antifouling [4], and corrosion protection [6]. The protection against corrosion of metals remains a crucial economic issue. Metals like copper, aluminum and steel have gained attention in industrial applications; however, no metal is protected from corrosion in different environments, so it is necessary to find solutions to protect these materials. In order to improve the corrosion resistance of these metals, common methods include: (I) adding a corrosion inhibitor [7]; (II) surface modification treatment [8]; (III) electrochemical protection [6]. These treatments provide good corrosion resistance in specific environments, but there are some limitations. Therefore, it is important to develop cost-effective, simple, non-toxic, and environmentally friendly surface treatment methods to prevent metal corrosion. Surface chemistry, including topology, is used to control surface wettability. For this mechanism, several techniques, such as hydrothermal method [5], electrodeposition [9], chemical vapor deposition [1] andthermal spraying [10] have been developed to achieve the surface wettability required for super hydrophiles. Among them, the electrodeposition technique presents controllable and suitable strategies for elaborating composite films on complex and diverse substrates, including adjusting the applied voltage and different electrolyte compositions [11]. In addition, it is a relatively less expensive and most practiced technique for creating roughness on the metal surface. For instance, Belamri et al. [12] reported the effect of annealing time on the morphological and structural characteristics of zinc oxide thin films grown on aluminum cathode substrates using electrodeposited technique. It has been observed that the shape and surface roughness of the as-prepared films had an

* e-mail: belamri.zehira@umc.edu.dz

impact on the results and the largest measured contact angle, of 97°, was obtained after annealing for 2 h at 500 °C. Lala et al. [13] studied the effect of compositional partitioning on microstructural evolution and corrosion behavior of Zn-Mo coatings (Mo: 2.8–6.5 wt%) electrodeposited on mild steel substrate. The authors showed that the corrosion resistance of Zn coating increased with Mo addition until Zn-4.2 wt% Mo, in addition, the incorporation of Mo resulted in the formation of Zn-Mo solid solution. Huang et al. [14] affirmed that superhydrophobic thin films have been fabricated on aluminum alloy substrates by electrophoretic deposition process using stearic acid functionalized zinc oxide (ZnO) nanoparticles suspension in alcohols at varying bath temperatures. It is shown that the atomic percentage of Zn and O, roughness and water contact angle of the thin films increase with the increase of the deposited bath temperature. The same authors in another work, prepared superhydrophobic aluminum surfaces by means of electrodeposition of copper on aluminum surfaces, followed by electrochemical modification using stearic acid organic molecules. A critical value of deposition potential of −0.6 V in combination with the stearic acid modification offers a surface roughness of 6.2 μm with a water contact angle of 157 °, resulting in superhydrophobic properties on the aluminum substrates [15]. Adding corrosion inhibitors or surface modification, are expensive and can lead to toxicity and environmental issues. So, it is important to develop cost-effective, simple, non-toxic, and environmentally friendly surface treatment methods to prevent metal corrosion. In our work, ZnO is chosen materials for their excellent physical properties and no toxicology material, using a low-cost and simple electroplating technique. In most scientific reports, the modification of ZnO films of coatings has been carried out in terms of the composition of the electrolyte solution, the temperature, the electric potential, the annealing treatment and the adjustment of the Zn:O ratio [16–19]. Among the elaboratment parameters, the concentration of the solution plays an important role in improvement of the crystallite size, texture coefficient and hydrophobicity of glass surfaces [20]. To our knowledge, there are a few articles in the literature describing the effect of molarity of ZnO thin film coating on aluminum metal substrate prepared by electrodeposition method.

In this context, the objective of the present work is to manufacture hydrophobic coatings on metallic aluminum substrates by adjusting the parameters of the electrodeposition and studying the morphology and surfaces wettability of thin layers obtained with different solutions molarity.

2 Experimental

Before the deposition of the Zn layer, the aluminum substrate undergoes mechanical polishing until a flat shape and a thickness of 2 mm are obtained. After that, it is ultrasonically cleaned for 15 min in two baths, one with distilled water and the other with ethanol. Zinc acetate dihydrate powder ($Zn(CH_3COO)_2.2H_2O$) precursor (VWR CHEMICALS Prolabo 99.8%), was first dissolved in distilled water to prepare the starting solution with different molarities (0.1, 0.2, and 0.3 M) for the deposition of Zn thin films. Aluminum substrate as cathode and platinum as anode were vertically immersed in the prepared solution. During the elaboration, various parameters were optimized in order to obtain uniform and adhesive deposits, are shown in Table 1. After deposition, the Zn films are thermally oxidized at 500 °C for 2 h in a tubular furnace. The current phases and their orientations were investigated using a PANALYTICAL empyrean diffractometer (XRD, Cu K_α radiation, $=1.540$ Å, scan speed of 0.164°/s, in the range from 10° to 80°). Raman spectra were registered using HORIBA LabRAM HR Evolution type spectrometer at room temperature with a monochromatic radiation source of 473 nm. The morphological and elemental analyses were performed using a Field Emission Gun Scanning Electron Microscope (SEM, Jeol FEG JSM-7100 F) equipped with an energy dispersive X-ray spectrometer (EDX). The roughness of deposited ZnO thin layers was measured by a PCE-RT 1200 model profilometer. The contact angle measurements are carried out 5 s after the deposit of a drop of water with a volume of 5 μL on the films produced using a LEYBOLD type light source (6 V, 30 W) and a projection lens which allows the static image of the drop displayed on a 30×30 cm^2 screen to be enlarged.

Table 1. Optimal conditions for the production of ZnO thin films.

Parameters	Optimized value
Zinc acetate solution concentration	0.1, 0.2, 0.3 M
Bath temperature	25 °C
Solution quantity	40 ml
Distance between the two electrodes	1.5 cm
DC Voltage	−10 V
Deposition time	15 min
Annealing temperature	500 °C

The flowchart in Figure 1 summarizes the experimental deposition procedure followed to elaborate our films.

3 Results and discussion

3.1 X-ray diffraction analysis

The identification of the electrodeposited layer and the thin film of ZnO structures formed after thermal oxidation at 500 °C were carried out by comparison with existing databases in the form of JCPDS files 03-065-3358/-01-079-2205 respectively. After the designation of the substrate peaks and that of Zn, the X-ray diffraction spectra of the prepared samples obtained at three molarities (0.1, 0.2, and 0.3 M) represent characteristic peaks of the compact hexagonal phase ZnO of Wurtzite structure, which proves that the ZnO was well synthesized in this present work (Fig. 2). The peaks intensity increases with increasing solution molarity, which is related to an increase in the crystallization level of the deposited layer due to the greater amount of Zn species present in the solution.

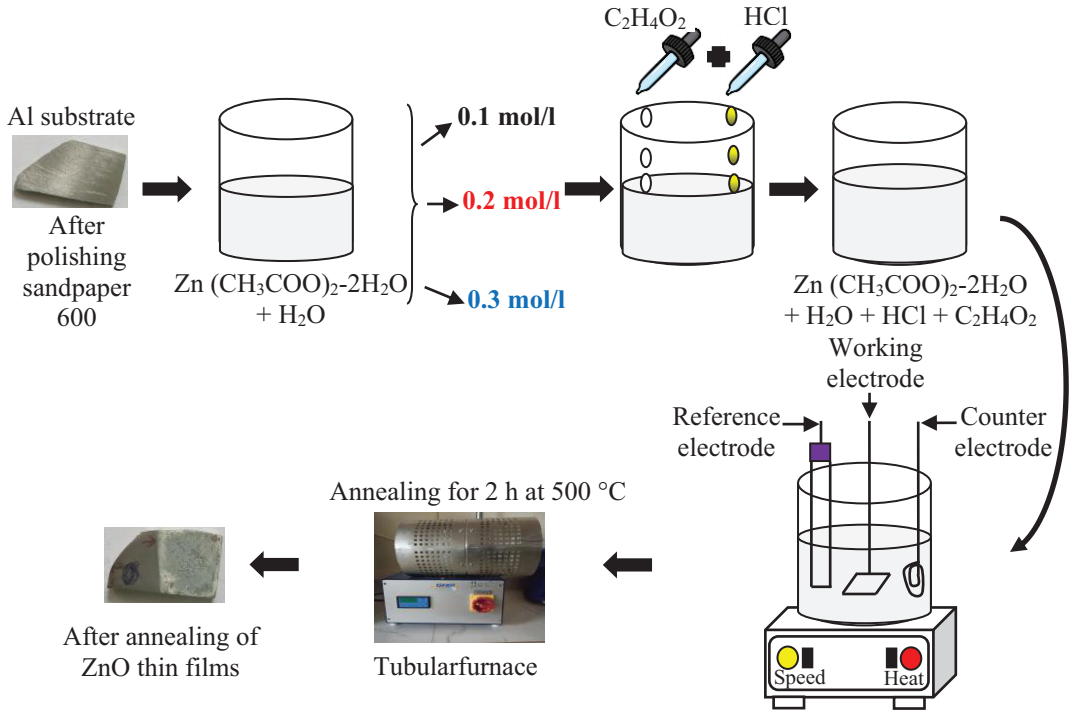

Fig. 1. Schematic diagram of ZnO thin films deposited with different molarity.

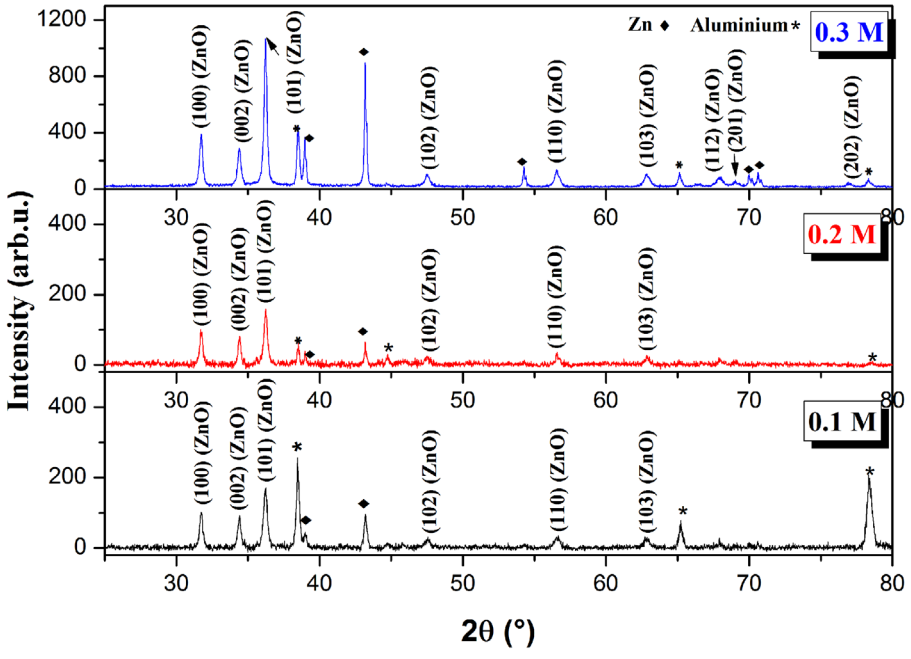

Fig. 2. XRD spectra of ZnO thin films prepared from the three molarities that are indicated on each spectrum.

With increasing molarity, the three diffractograms show a main peak of this structure located at 36.2151°, 36.2356°, and 36.2242°, respectively, highlighting a privileged orientation of ZnO structure growth along the crystallographic axis (101). The peak (101) narrows with the increase in molarity, which lets us, think that the average crystallites size forming the layer increases with the increase in the solution molarity. The average crystallites size was evaluated according to the most intense peak (101) using the flowing Scherrer's relationship [21–23].

$$D = \frac{0.9\lambda}{\beta \cos\theta} \quad (1)$$

Table 2. Average crystallites size, a, c and texture coefficient ($TC_{(hkl)}$) values of prepared ZnO thin layers.

Molarity, (mol/l)	$2\theta_{100}$ (°)	$2\theta_{101}$ (°)	$2\theta_{002}$ (°)	FWHM	D, (nm)	a, (Å)	c, (Å)	$TC_{(hkl)}$
0.1	31.7331	36.2151	34.3971	0.3342	25	3.2533	5.2102	0.893
0.2	31.7383	36.2356	34.4058	0.3044	27	3.2528	5.2090	0.911
0.3	31.7288	36.2242	34.3962	0.2606	32	3.2538	5.2104	1.368

where, is the X-ray wavelength (0.15406 nm for Cu Kα radiation), β is the full width at half maximum (FWHM) of the peak corresponding to the (101) orientation and θ is the Bragg angle corresponding to the (101).

Table 2 displays the obtained results. From the obtained results, it is noted that the crystallite size increases with the increase in molarity; this may be due to the increase in the number of Zn ions reaching the substrate. A higher condensation of the Zn atoms accompanied a faster nucleation of the crystallites, which leads to an increase in their size. This indicates the enhancement of the ZnO thin layer crystallinity, which is achieved with 0.3 M.

There is also a shift of the most intense peak (101) of the ZnO layer towards higher values than the normalized one (36.215°). In order to explain this shift, one can calculate the lattice parameters a and c using the following relations valid for the hexagonal structure [24]:

$$a = \frac{\lambda}{\sqrt{3} * \sin\theta} \tag{2}$$

$$c = \frac{\lambda}{\sin\theta} \tag{3}$$

where, λ: is the X-ray wavelength (1.5406 Å) and θ: is diffraction angle of (100) peak for a parameter and of (002) peak for c parameter.

Table 2 displays the obtained results.These values are slightly different from those of the normalized ZnO lattice parameter values, which are: $a = 3.253$ Å and $c = 5.213$ Å. This indicates that these layers are in a compression state parallel to their growth direction, which may be due to the difference in thermal expansion coefficients between the deposited material and the aluminum substrate.

When the crystal lattices of the substrate and the layer perfectly accommodate each other, a crystallographic relationship appears at the interface. A deformation due to the disagreement of the lattice parameters of the materials can also be caused by this accommodation. This type of deformation generates coherence stresses in the two contacting materials. The stress state in the elaborated ZnO layers can be determined using XRD spectra. The biaxial stress e_{zz} along the c axis perpendicular to the plane of the substrate is calculated from the c parameter [25]:

$$e_{zz} = \frac{C_{film} - C_0}{C_0} * 100 \tag{4}$$

where, C_{film}: lattice parameter of the deposited layer and $C_{JCPDS} = C_0 = 5.213$ (Å).

Table 3. e_{zz} and σ values for deposited ZnO thin films of various molarities.

Molarity, (mol/l)	e_{zz}, (%)	σ, (GPa)
0.1	−0.052	0.120
0.2	−0.076	0.178
0.3	−0.049	0.115

We can confirm the type of stress that the layer undergoes by studying the sign of e_{zz} parameter. The calculation results (Tab. 3) show that the e_{zz} has a negative sign, which confirms that this layer undergoes a compressive stress parallel to the direction of its growth.

The residual stress σ parallel to the surface of the layer is expressed by the following relation [25]:

$$\sigma = \frac{2C_{13}^2 - C_{33}(C_{11} + C_{12})}{2C_{13}} * \frac{C_{film} - C_0}{C_0} \tag{5}$$

where, c_{ij} is the elastic constant for a monocrystalline ZnO structure ($c_{13} = 104.2$ GPa, $c_{33} = 213.8$ Gpa, $c_{11} = 208.8$ Gpa and $c_{12} = 119.7$ Gpa)[24].

$$\sigma(GPa) = -233 * e_{zz}. \tag{6}$$

The calculated values of σ for the samples of different molarities are presented in Table 3. It's noted that all these values have a positive sign, indicating that the ZnO layers are under a tensile stress perpendicular to the c axis.

The texture coefficient $TC_{(hkl)}$which can be evaluated using the following relationships. Equation (7) [26], is calculated in this work:

$$TC(hkl) = \frac{\frac{I_{(hkl)}}{I_{0(hkl)}}}{\frac{1}{N}\sum\frac{I_{(hkl)}}{I_{0(hkl)}}} \tag{7}$$

where: $TC_{(hkl)}$: Texture coefficient of (hkl) plane, $I_{(hkl)}$: XRD peak intensities obtained from the films, $I_{0(hkl)}$: Intensities of the standard diffraction pattern (JCPDS card 01-079-2205) and N: Number of considered diffraction peaks.

The obtained calculus (Tab. 2) shows that the texture coefficient of the (101) peak for ZnO thin films increases from 0.893 to 1.368 as the solution molarity increases from 0.1 to 0.3 M. This indicated that the crystallites are preferentially oriented along the (101) plane. Also, the intensity of the (101) peak gradually increases with the

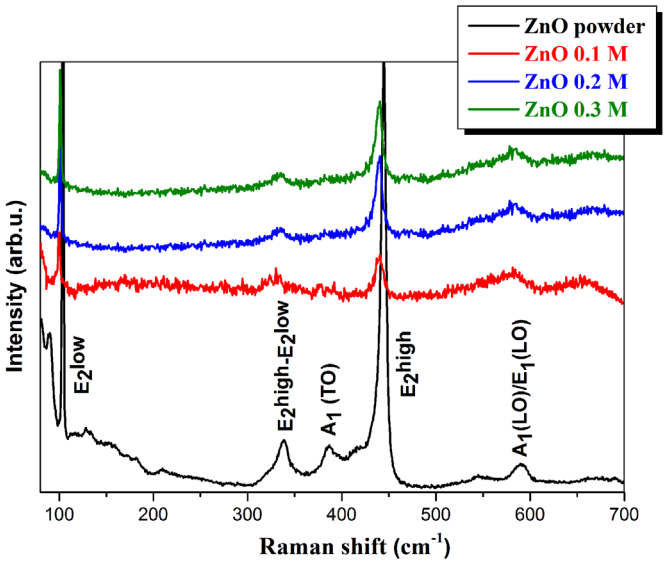

Fig. 3. Raman spectra of ZnO thin films obtained from 0.1, 0.2, and 0.3 M (ZnO powder as reference bulk state material).

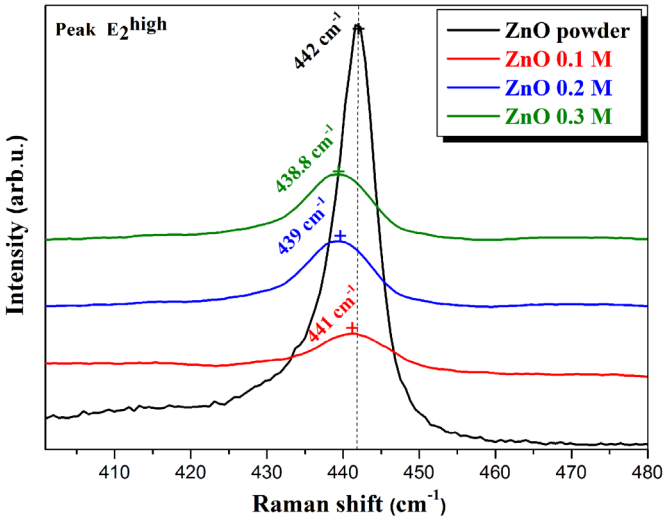

Fig. 4. Superposition of the Raman E_2^{high} peak of studied ZnO thin films.

solution molarity which concluded that the increase in solution molarity enhances the crystallinity of the studied thin films.

3.2 Raman spectroscopy analysis

To complete the structural properties study of the elaborated ZnO thin films, Raman spectroscopy was used in this present work. Raman spectroscopy can inform us about the structural properties of the studied materials, their stress states, and the determination of the different phases through the identification of the different vibration modes of the crystal lattice. Thus, we can know the stress state present in the studied material by observing the displacement of the peak position in comparison with the values of the material in bulk state. In this present work, commercial ZnO powder is used as a reference (bulk state material).

The obtained spectra of the studied samples (Fig. 3) are similar to those of massive ZnO and consist of five peaks corresponding to E_2^{Low}, E_2^{high}–E_2^{Low}, A1(TO), E_2^{high}, and A1(LO) /E1(LO) modes of the ZnO phonons of hexagonal structure [27]. The presence of all these peaks with variable intensities depends on the deposited solution molarity. These the three spectra present two intense peaks around 100 cm^{-1}, which correspond to the E_2^{Low} mode associated with the vibration of the zinc atoms lattice [27], and at 440 cm^{-1}, which correspond to the E_2^{high} mode which is attached to the vibration of the sub-lattice of oxygen atoms in the ZnO crystal [28]. These two representative modes of Wurtzite ZnO structure with good crystalline quality.

It is known that E_2^{high} phonon Raman spectroscopy plays an important role in studying the residual stress in ZnO crystals because the stress induced in Wurtzite structure crystals affects the frequency of E_2 phonons. A decrease in the E_2^{high} phonon frequency is attributed to tensile stress, while its increase is attributed to compressive stress [29]. Figure 4 clearly shows the shift of the E_2^{high} phonon peak towards low frequencies for the three studied thin films, its value is slightly lower than that of bulk ZnO (442 cm^{-1}) which suggests that the films were under slight tensile stress.This confirms the calculation results obtained from the residual stress in this present work.

3.3 Morphology and wettability analysis

There are varieties of ZnO nanostructures that have been discovered in the form of nanorods, nanotubes, nanobelts, nanosprings, nanospirals, nanorings, and many others [30,31]. Figures 5 – 7 show the FEG-SEM images and the images of water droplet on the surface of elaborated ZnO thin films with different molarity. They clearly illustrate that the grain size of studied ZnO layers and their morphology depends strongly on the concentration of solution.

If the solution concentration is 0.1 M, the films are relatively compact (Fig. 5a). The microstructure presents a mixture of spherical granular with an average size of 40 nm and a large compact grains with an average size of 200 nm. According to the literature [16,22], contact angle washers were well associated with film roughness. So, Grain growth due to aggregation during deposition causes an increase in the roughness of the film. This leads to a contact angle with water of this surface of 128.43° (Fig. 5c) and the surface is considered hydrophobic. The surface morphology changed as the solution concentration increased. The ZnO sample of 0.2 M exhibits a compact morphology with micrometric granular attached to each other with an average size of 200 nm, well-defined grain boundaries and few nanorods (Fig. 6a). The droplet shape on this surface was more specific (Fig. 6c).This indicates that the structure of the ZnO film prepared with solution of 0.2 M is hydrophobic with a larger contact angle (135.72°) than that the film prepared with 0.1 M (128.43°). According to the obtained results of roughness measurements (Tab. 4), we observe that the roughness values are well linked to the contact

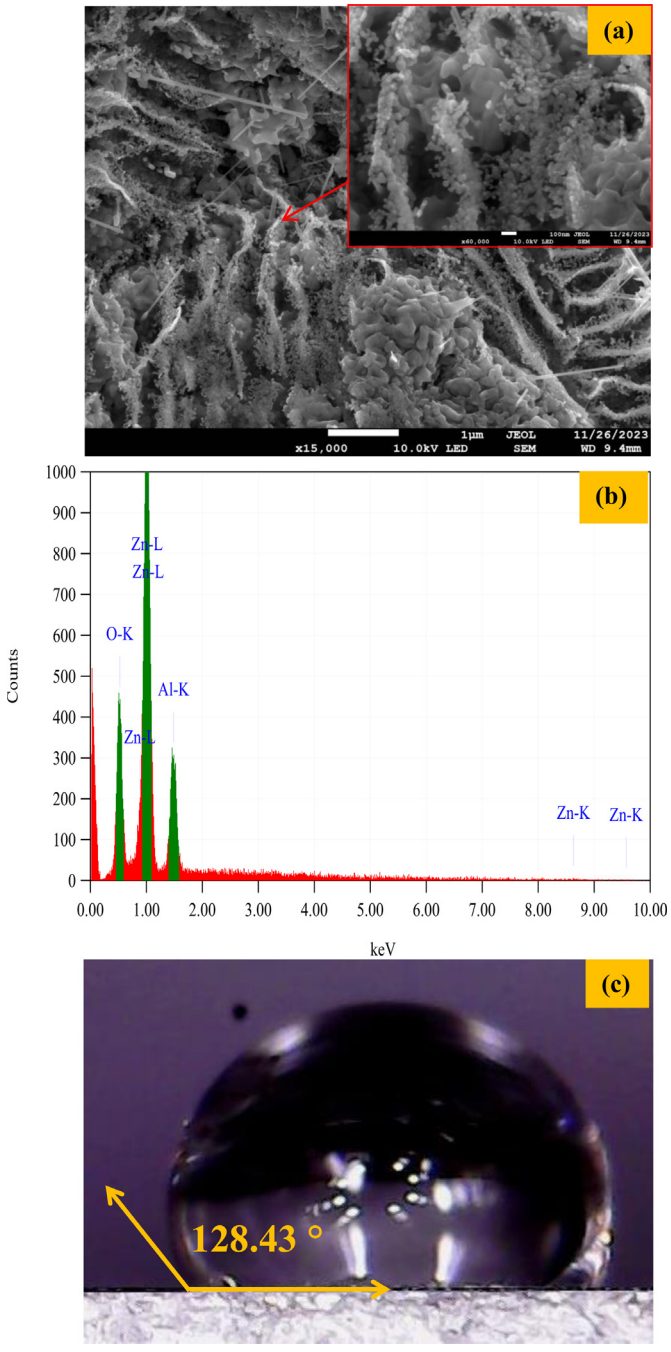

Fig. 5. FEG-SEM image of ZnO thin film with 0.1 M, inset shows a high magnification image (a), corresponding EDS with appropriate indexing (b), and contact angle with water of the ZnO coating (c).

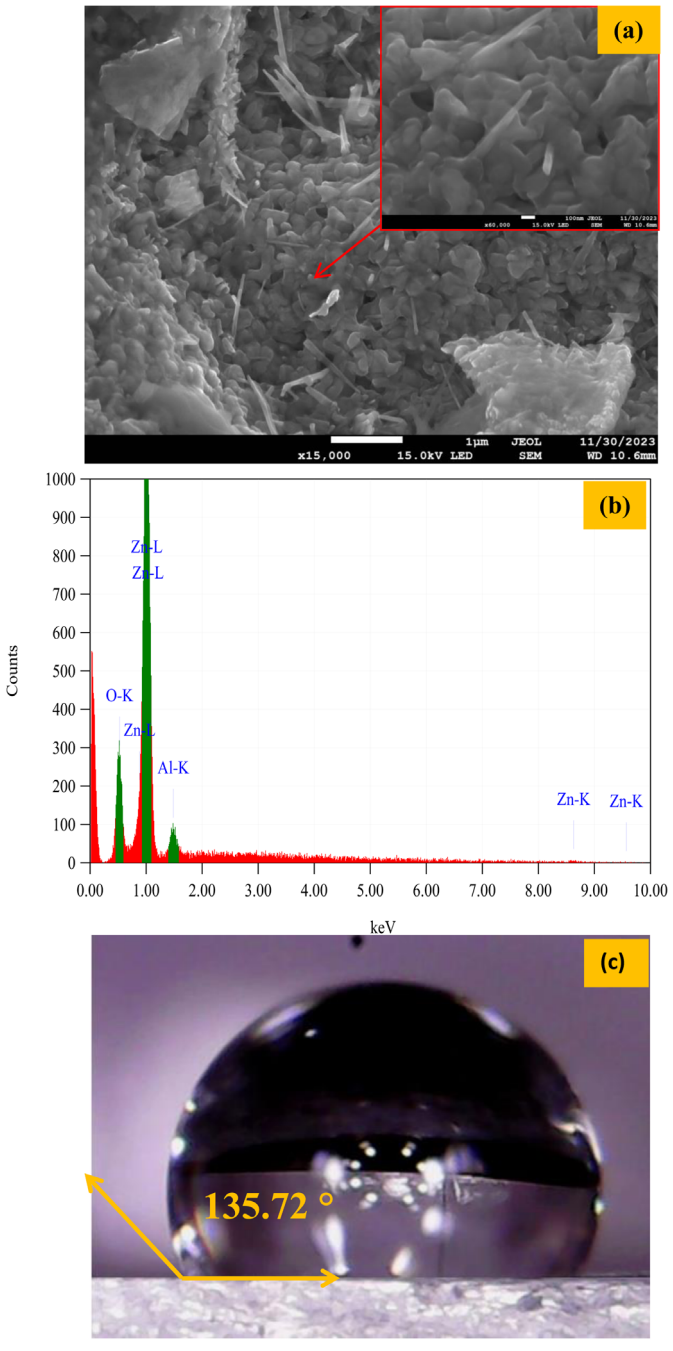

Fig. 6. FEG-SEM image of ZnO thin film with 0.2 M, inset shows a high magnification image (a), corresponding EDS with appropriate indexing (b), and contact angle with water of the ZnO coating (c).

angle. So, we can conclude that the highest roughness presents the highest contact angle. The same result was observed by Huang et al. [15] by studying of copper films on aluminum surfaces deposited by electrodeposition. Therefore, the rougher surface of 7.653 µm corresponds to sample prepared with 0.2 M due to grain growth caused by aggregation during deposition. The amount of solute in the solution increases as the concentration increases, and consequently the electrostatic interaction between the solute particles becomes more significant, which increases the chance of the solute coming together to form a grain, so, the film surface also comes to be rougher. As the concentration increases, the film morphology changed, where the structure of the 0.3 M sample contains nanofibers (Fig. 7a). The droplet shape at this surface has flattened (Fig. 7c) and the contact angle decreases to 87.17°. This decrease may be due to the formation of a large number of ZnO nanofibers and the surface becoming

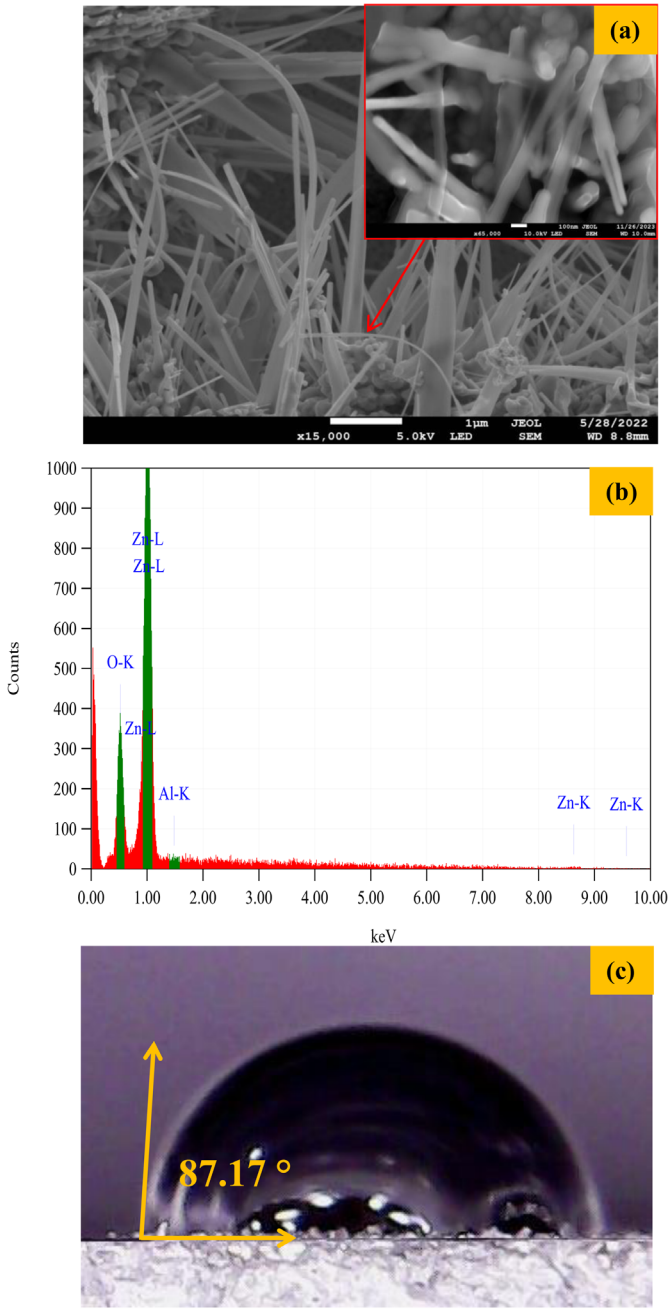

Fig. 7. FEG-SEM image of ZnO thin film with 0.3 M, inset shows a high magnification image (a), corresponding EDS with appropriate indexing (b), and contact angle with water of the ZnO coating (c).

hydrophilic. Elemental analysis performed by EDS shows the presence of zinc and oxygen in the three elaborated ZnO thin films.

4 Conclusion

The objective of this present work is the deposition and characterization of hydrophobic coating films of zinc oxide for different molarity of solution on metallic aluminum substrates for different concentration of solution by the electrodeposition technique with a view to obtaining materials with good wettability properties of a solid surface. X-ray diffraction reveals a polycrystalline nature of the hexagonal ZnO phase of Wurtzite structure for all the elaborated thin films, with a preferential crystallite orientation following (101). The calculated microstructure parameters of the studied thin films such as crystalline size (D) and texture coefficient ($TC_{(hkl)}$), showed that the crystallites size increases with increasing solution molarity. So, the better crystalline quality is obtained with prepared solution of 0.3 M. The difference in thermal expansion coefficients between the deposited material and the substrate as well as the disagreement of their lattice parameters lead to the existence of stresses in the two contacted materials. The layers undergo a compressive stress parallel to the direction of their growth and another tensile stress perpendicular to the c axis. The Raman spectroscopy analysis confirms the results obtained by XRD, where the Raman spectra of elaborated ZnO thin films consist of different hexagonal ZnO phonon modes. The morphological study of the elaborated ZnO thin films surface has been also studied in this work. It clearly illustrates the formation of micro/nanometric grains distributed more or less uniformly on the surface and strongly depends on the concentration of solution. The water droplet shape on these layers related to their morphologies where the best hydrophobicity with a contact angle of 135.72° is achieved with a compact granular morphology attached to each other. This is carried out with a 0.2 M molarity solution possesses a larger roughness. The contact angle washers were well associated with film roughness. In this study, the film prepared at 0.2 M on metallic aluminum substrate using a simple and cost-effective electrodeposition technique demonstrates optimal properties for preventing metal corrosion.

Table 4. Roughness and the contact angle as a function of solution molarity for the deposited ZnO samples.

Molarity, (mol/l)	Roughness, (µm)	Contact angle, (°)
0.1	2.233	128.43
0.2	7.653	135.72
0.3	0.526	87.17

Funding

This research received no external funding.

Conflicts of interest

The authors have nothing to disclose.

Data availability statement

No data was used for the research described in the article.

Author contribution statement

The experimental work and the writing of the manuscript were done by Zehira Belamri. The experimental protocols, the data analysis and the interpretation of the results were performed by Zehira Belamri, Warda Darenfad and Noubeil Guermat. Zehira Belamri and Warda Darenfad contributed to the extensive revising of the manuscript. All authors discussed the results and commented the manuscript. The authors declare no competing financial interests.

References

1. J. Fu, Y. Sun, Y. Ji, J. Zhang, J. Mater. Process. Technol. **306**, 117641 (2022)
2. T.P. Rasitha, D. Nanda Gopala Krishna, C. Thinaharan, S.C. Vanithakumari, J. Philip, Prog. Org. Coat. **172**, 107076 (2022)
3. N. Hassan, M.M. Fadhali, S. Al-Sulaimi, M.S. Al-Buriahi, K.M. Katubi, Z.A. Alrowaili, M.A. Khan, R. Shoukat, Z. Ajmal, F. Abbas, Z.E. Humma, U.E. Kalsoom, R.T. Rasool, J. Mol. Liq. **383**, 122085 (2023)
4. C. Xie, C. Li, Y. Xie, Z. Cao, S. Li, J. Zhao, M. Wang, Surf. Interfaces. **22**, 100833 (2021)
5. H. Peng, H. Yang, X. Ma, T. Shi, Z. Li, S. Xue, Q. Wang, Colloids Surf. A Physicochem. Eng. Asp. **643**, 128800 (2022)
6. M. Saeedikhani, S. Wijesinghe, D.J. Blackwood, Corros. Sci. **163**, 108296 (2020)
7. A. Fateh, M. Aliofkhazraei, A.R. Rezvanian, Arab. J. Chem. **13**, 481 (2020)
8. G. Xu, K. Wang, X. Dong, L. Yang, M. Ebrahimi, H. Jiang, Q. Wang, W. Ding, J. Mater. Sci. Technol. **71**, 12 (2021)
9. Z. Belamri, W. Darenfad, N. Guermat, J. Nano-Electron. Phys. **15**, 02026 (2023)
10. B. Subeshan, R. Asmatulu, Eng. Fail. Anal. **139**, 106437 (2022)
11. M. Moradi, R. Saidi, B. Hoomehr, K. Raeissi, Ceram. Int. **49**, 9239 (2023)
12. Z. Belamri, L. Boumaza, S. Boudjadar, Phys. Scr. **98**, 125949 (2023)
13. S.R.F. Lala, A.P. Singh, S. Singh, S.C. Tiwari, C. Srivastava, Materialia. **27**, 101709 (2023)
14. Y. Huang, D.K. Sarkar, X.-G. Chen, Appl. Surf. Sci. **327**, 327 (2015)
15. Y. Huang, D.K. Sarkar, X.-G. Chen, Nano-Micro. Lett. **3**, 160 (2011)
16. G. Acikbas, H. Hindi, J. Inorg. Organomet. Polym. Mater. **34**, 419 (2024)
17. Omnia A.A. El-Shamy, M.A. Deyab, Mater. Lett. **331**, 133402 (2023)
18. S. Özcan, G. Açıkbas, N. Çalıs Açıkbas, Appl. Surf. Sci. **438**, 136 (2023)
19. R. Somoghi, V. Purcar, E. Alexandrescu, I.C. Gifu, C.M. Ninciuleanu, C.M. Cotrut, F. Oancea, H. Stroescu, Coatings **11**, 444 (2021)
20. N.L. Tarwal, P.S. Patil, Appl. Surf. Sci. **256**, 7451 (2010)
21. W. Darenfad, N. Guermat, K. Mirouh, J. Nano-Electron. Phys. **13**, 06016 (2021)
22. N. Guermat, W. Darenfad, K. Mirouh, N. Bouarissa, M. Khalfallah, A. Herbadji, Eur. Phys. J. Appl. Phys. **97**, 14 (2022)
23. M. Khalfallah, N. Guermat, W. Daranfed, N. Bouarissa, H. Bakhti, Phys. Scr. **95**, 095805 (2020)
24. J. Zhao, J. Ni, X. Zhao, Y. Xiong, J. Wuhan Univ. Technol. Mater. Sci. Ed. **26**, 388 (2011)
25. M. Chen, Z.L. Pei, C. Sun, L.S. Wen, X. Wang, J. Cryst. Growth. **220**, 254 (2000)
26. N. Khedmi, M. Ben Rabeh, D. Abdelkadher, F. Ousgi, M. Kanzari, Cryst. Res. Technol. **50**, 69 (2014)
27. U. Ozgur, Y.I. Alivov, C. Liu, A. Teke, M.A. Reshchikov, S. Dogan, V. Avrutin, S.J. Cho, H. Morkoc, J. Appl. Phys. **98**, 041301 (2005)
28. B. Hadžić, N. Romčević, M. Romčević, I. Kuryliszyn-Kudelska, W. Dobrowolski, U. Narkiewicz, D. Sibera, Opt. Mater. **58**, 317 (2016)
29. E. Muchuweni, T.S. Sathiaraj, H. Nyakotyo, Heliyon **3**, e00285 (2017)
30. W. Darenfad, N. Guermat, K. Mirouh, J. Mol. Struct. **1286**, 135574 (2023)
31. N. Guermat, W. Daranfed, I. Bouchama, N. Bouarissa, J. Mol. Struct. **1225**, 129134 (2021)

Cite this article as: Zehira Belamri, Warda Darenfad, Noubeil Guermat, Molarity dependence of solution on structural and hydrophobic properties of ZnO nanostructures, Eur. Phys. J. Appl. Phys. **99**, 10 (2024)